RSC Advances

ROYAL SOCIETY OF CHEMISTRY

www.rsc.org/advances

Effect of defects and film thickness on the optical properties of ZnO/Au hybrid films

K. Saravanan,[1*] R. Krishnan,[2] S. H. Hsieh,[1] H. T. Wang,[3] Y. F. Wang,[1] W. F. Pong,[1] K. Asokan,[4] D. K. Avasthi[4] and D. Kanjilal[4]

[1]Department of Physics, Tamkang University, Tamsui - 251, Taiwan

[2]Materials Science Group, Indira Gandhi Centre for Atomic Research, Kalpakkam - 603102, India.

[3]Department of Physics, National Tsing Hua University, Hsinchu - 30013, Taiwan.

[4]Materials Science Group, Inter-University Accelerator Centre, New Delhi - 110067, India.

Abstract

Electronic structure and optical properties of ZnO(*y* nm)/Au(10 nm) hybrid films, with *y* = 20, 50 and 150, have been investigated for effective coupling of surface plasmon resonance (SPR) of Au nanoparticles (NPs) with ZnO band structure to enhance their optical property. The films have been synthesized by pulsed laser deposition method and studied by UV-Visible absorption, Raman, Photoluminescence, and X-ray absorption near-edge structural analyses. The effect of defects on coupling of SPR with ZnO band structure has been discussed based on optical and electronic structural studies. The local electronic structure analysis at O *K*-edge reveals that, in thinnest film more unoccupied states are introduced in ZnO due to hybridization of O 2*p* - Au 5*d*/6*s* orbitals. The increased density of states causes the enhanced optical properties of ZnO/Au hybrid films via increasing the population at the conduction band of ZnO. Our experimental findings demonstrate that in thickest film, the exponential decay of SPR induced local field and defects are the main factors affecting the coupling of SPR with the ZnO band structure.

[*]**Electronic mail:**
saravananmsc05@gmail.com

Introduction

In recent years, semiconductor/metal hybrid thin films have received intense research interest owing to their potential application in future electronic and optoelectronic devices.[1-3] These plasmonic devices have made major advances to solve the low light-emission efficiency problem in the conventional light emitting diodes (LEDs)[1] and to enhance the sensitivity of ultraviolet (UV) photodetectors.[3] The surface plasmon resonance (SPR), unique property of noble metal clusters, is the main reason for enhanced optical and electronic properties of such plasmonic composites.

In the present work, we focus on the optical and electronic structural properties of ZnO/Au hybrid system since ZnO, with its wide direct bandgap (~ 3.36 eV) and high exciton binding energy (~ 60 meV), is recognized as one of the most promising material for optoelectronic applications.[4,5] ZnO films typically exhibit photoluminescence (PL) emission in the visible and UV region. The UV emission of ZnO is due to band-to-band transition whereas the visible emission (~ 2.3 eV) is related to defects like oxygen vacancies.[6,7] As the enhanced UV emission with suppressed visible emission of ZnO is essential for UV LED, laser diode applications, the hybrid structures of ZnO/metal have intense research interest to enhance the optical properties of ZnO.[8-11] SPR of Au nanoparticles (NPs) can produce a strong electromagnetic field at the surface and has been used in variety of applications starting from biosenors to solar cells.[12-15] However, only few research groups have shown considerable enhancement of PL emission in Au-ZnO composites.[10,11,13] and the mechanism for the enhancement is still under debate. The role of defects and film thickness on the hybridization of Au-ZnO band structures, particularly the optical properties, is unclear in the literature. This is mainly due to the complicated nature of SPR effect of Au nanoparticles, which depends on the size, shape and environment.[16] Hence, a systematic study is essential for better

understanding of ZnO/Au system, and realization of coupling of evanescent wave of surface plasmons with the ZnO band electrons.

In this work, the effect of SPR of Au NPs on the electronic structure of ZnO in ZnO/Au hybrid films with different thickness of ZnO has been discussed in detail with the aid of UV-Visible absorption, Raman, PL and X-ray absorption near edge structure (XANES) studies. The thinnest ZnO film shows enhanced UV emission and suppressed visible emission in the presence of Au NPs, while the PL emission of thickest films is in-sensitive to the Au NPs. The local electronic structure analysis at O *K*-edge reveals that, in thinnest film more unoccupied states are introduced in ZnO due to hybridization of O 2*p* and Au 5*d*/6*s* orbitals. The increased density of states causes the enhanced optical properties of ZnO/Au hybrid films via increasing the population at the excited state of ZnO, whereas the exponential decay of SPR induced local field and defect density in thickest film are the main factors affecting the coupling of SPR with the ZnO band structure.

Experimental details

The ZnO(*y* nm)/Au(10 nm) hybrid films were prepared by pulsed laser deposition method on quartz substrates. First, Au film (~10nm) was deposited at room temperature under high vacuum condition and subsequently ZnO film, with different thicknesses (*y* = 20, 50 and 150), was deposited on these samples in oxygen atmosphere at a pressure of 1.5 mbar at 350°C. For comparison, ZnO films of same thicknesses, under identical conditions, have also been prepared without Au film. The elemental composition and thickness of the synthesized films were measured by Rutherford backscattering spectrometry (RBS). 2 MeV He^+ ions from 1.7 MV Pelletron accelerator (NEC, USA) was used for RBS measurements. The cross-sectional view of the films has been analyzed using transmission electron microscope (TEM). Optical properties of the synthesized films have been studied by UV–visible absorption, PL and resonant Raman spectroscopic measurements. The XANES experiments were performed

at the BM-(H-SGM) XAS - 20A and SWLS-01C beamlines at National Synchrotron Radiation Research Center (NSRRC), Hsinchu, Taiwan. The spectra were recorded in total electron yield (TEY) or total fluorescence yield (TFY) mode at glancing incident angle (70°).

Results and Discussion

A. Structural and Compositional analysis

Fig. 1 shows the RBS spectra of ZnO(*y* nm)/Au(10 nm)/Qz and ZnO(*y* nm)/Qz samples. The signal from Au, Zn, O and Si are clearly seen in the RBS spectra. The peak width and backscattering yield of the RBS spectra are proportional to the thickness and concentration of the corresponding element in the sample.[17] The RBS spectra have been simulated using SIMNRA software[18] to estimate the film thicknesses and the samples are categorized as thickest films, thin films and thinnest films according to the ZnO film thickness, y = 150, 50 and 20, respectively. The thickness of Au film is kept constant ~10 nm. After the Au deposition the surface topography of randomly selected sample is analyzed by atomic force microscopy (AFM), (inset-I in Fig.1). The estimated Au cluster size is in the range 7 - 10 nm. The cross-sectional view of the synthesized films have been analyzed by TEM and the typical TEM images are shown in the insets of Fig.1. It is clear that the deposited Au film formed as nanoparticles of size ~10 nm at the interface between the substrate and ZnO film.

The glancing angle XRD patterns of thinnest and thickest set of films are shown in Fig. 2(a). In all these samples, the peak at 34.42° is the diffraction from the (002) planes of the hexagonal wurtzite ZnO crystallites (JCPDS #361451). The strong peak scattered from the (002) plane indicates that the films are preferably oriented along c-axis. Broadening of (002) peak in thinnest samples may due to narrowing of crystallite size with decreasing of film thickness. The XRD pattern corresponding to the *fcc* Au nanocrystallites is also observed in ZnO film deposited with Au film. Since, the intensity of the XRD peak is weak in the thinnest films, we could not get more information from them. However, the XRD results

confirm the presence of Au and do not provide any evidence of oxides of Au in case of ZnO/Au films. Furthermore, the Raman studies of these films confirm that the ZnO films are of wurtzite structure. Fig. 2(b) shows the resonant Raman scattering spectra of all synthesized films. The longitudinal optical (LO) phonon modes namely 1 LO and 2 LO have been observed in all the samples around 570 and 1150 cm^{-1}, respectively. These modes are corresponding to the wurtzite structured ZnO films.[19-21] In thin and thinnest sets, the samples ZnO/Au/Qz show enhanced intensity of 1 LO and 2 LO modes in comparison with ZnO/Qz samples. This enhancement is due to the local field induced by SPR of Au NPs.[22] Generally, the Au thin film evolved as isotropic NPs by thermal induced dewetting process when heated to a temperature above 300°C.[23] In the present work, the substrate temperature together with the laser ablation energy leads to the evolution of nearly spherical shape Au NPs (as seen in TEM analysis). The inset of Fig. 1(b) displays the intensity ratio of 2LO/1LO modes. Generally, these LO modes are associated with the defects like O vacancy, Zn interstitial or their complexes in the film.[24] Further, the 2LO/1LO ratio is mainly correlated to the electron-phonon coupling (EPC) via Fröhlich interaction caused by electric field.[25] In thin and thinnest set of ZnO/Au/Qz films, the 2LO/1LO ratio is less in comparison with ZnO/Qz. This indicates that the EPC is strong in ZnO/Qz films and weak in ZnO/Au/Qz films. The weak EPC in ZnO/Au/Qz films may be due to the enhanced electric field induced by SPR of Au NPs. However, in thickest set of films, the 2LO/1LO ratio is insensitive to the Au NPs. This is attributed to weak strength of SPR induced field as the strength decays exponentially away from the Au NPs.[26]

B. Optical studies

Fig. 3(a) shows the UV-visible absorption spectra of all samples. All samples have shown an absorption peak around 365 nm, which is correspond to the band gap of ZnO (3.4 eV).[12]

The absorption intensity decreases with the decrease of ZnO film thickness. According to the Beer-Lambert law,[27] the absorbance can be written as,

$$A = log(I_0/I) = \varepsilon cl \quad (1)$$

where I_0 is the intensity of the incident light at a given wavelength, I is the transmitted intensity, L is the pathlength through the sample, c is the concentration of absorbing species. ε is the molar absorptivity. Hence in the present work, the thickest film exhibits enhanced absorption because of increased pathlength. In addition to the absorption peak at 365 nm, the thickest ZnO film exhibits a broad absorption in the region 500 - 800 nm. This is due to the presence of defects, which creates defects levels in the sub-bandgap region.[28] However, this peak has not been observed in thin and thinnest ZnO films. This may be due to less number of defects in these films. Due to large volume fraction, the defect band is clearly observed in thickest film, whereas, the Raman and PL analyses confirm the presence of defects in all the films. Further, these ZnO/Au/Qz samples exhibit an absorption peak around 600 nm, which is attributed to the SPR of Au NPs in the vicinity of ZnO.[12]

Fig. 3(b) shows the UV PL emission spectra. In thickest films, the band edge emission intensity is same for both ZnO/Au/Qz and ZnO/Qz samples. This indicates that the SPR of Au NPs has no effect on the emission of ZnO film. This is observation is consistent with reports available in literature.[8,13,29] However, in case of thin sets, the ZnO/Au/Qz film shows enhanced emission in comparison with the ZnO/Qz film, and the enhancement is more in thinnest ZnO film. This enhancement is due to the strong interaction between ZnO electronic structure and SPR of Au NPs. This observation is different from the earlier reports and confirms the strong effect of SPR on ZnO PL emission. Further, the thickest set of samples exhibit a broad visible emission (Fig. 3(c)). The intensity of this peak is same for both ZnO/Au/Qz and ZnO/Qz samples. However, in thin and thinnest sets, ZnO/Au/Qz films show a suppressed visible emission in comparison with ZnO/Qz films. Fig. 3(d) displays the

enhancement ratio of UV emission (area under the peak) and suppression ratio of visible emission. It is seen that the estimated ratio of the suppressed visible emission is almost equal to the enhancement of UV emission. This indicates that, in the presence of Au NPs, the population (excited electrons) of ZnO conduction band increases and they radiatively recombine with the valence band holes. The suppression of defect emission, in the presence of Au NPs, may due to the combined effect of SPR of Au NPs and passivation of the ZnO surface states.[30] However, in case of thickest ZnO film, the SPR has no effect on either UV or visible PL emission. When the thickness is large, the coupling effect of SPR to ZnO band electrons vanishes as only the electron/hole pairs near to the Au NPs can effectively couple to increase the internal quantum efficiency for the enhanced PL emission.[31] Moreover, the PL intensity of ZnO/Au hybrid film depends on the total attenuation of band edge emission, determined by scattering and surface defects, and the enhancement effect caused by SPR of Au NPs.[32] Under O-rich growth conditions, the ZnO film may have some native acceptor defects like Zn vacancy (V_{Zn}) and interstitial oxygen (O_i) as they have low energy formation energy.[33] The Raman and UV- visible absorption studies also confirm the existence of defects in these films. These defects could alter the density of states in the band structure and recombination mechanism of PL emission. Hence, the excited electrons are trapped in these defect levels due to strong EPC. In such case the excited electron first emits phonons to decay to a lower energy level, and from there it emits a photon (defect emission) to recombine with the valence band holes.[34-36] Hence the possible reasons for poor enhancement in thickest films are (i) weak strength SPR induced local field as away from the Au NPs surface, and (ii) the surface defect (traps) density in the ZnO film which will also quench the band-edge emission of ZnO.

C. Electronic structural studies

In order to understand the effect of defects and film thickness on the coupling of SPR with the ZnO band electrons, XANES measurements have been performed and are shown in Fig. 4. The Zn $L_{3,2}$-edge XANES features were found to be same in all the samples (not shown here). Fig. 4(a) shows the O *K*-edge XANES spectra and the features observed at 533.7, 538.5, 542 and 544.5 eV, are labeled as A, B, C and D, respectively. The features in the region 530 - 539 eV are attributed to O 2*p* states hybridized with Zn 3*d*4*s*/Au 5*d*, while the features in the region 539 - 550 eV are attributed to O 2*p* states hybridized with Zn 4*p*/Au 5*d*6*s*.[37] Specifically, the features at 533.7 and 538.5 eV are correspond to the transition from O 1*s* to O $2p_z$ and $2p_{x+y}$ orbitals, respectively.[38] The thin and thinnest ZnO films have shown enhanced features A and D in the presence of Au NPs. The enhanced intensity is due to more unoccupied states are introduced in O 2*p* states by Au NPs. However, the intensities of feature B and C are less in comparison with ZnO/Qz samples. Interestingly, the O *K*-edge features of thickest ZnO/Au/Qz film are different from the features of thinnest film. In thickest ZnO/Au/Qz film, the intensities of feature A and D are almost same as ZnO/Qz while the B and C features are higher than ZnO/Qz. These observations indicate that, the thickness of ZnO film has significant influence on the hybridization of O 2*p* and Au 5*d*/6*s* orbitals in ZnO/Au hybrid structures.

Since the Raman and PL measurements were carried out with UV laser excitation, the XANES measurements with additional UV laser (λ_{exc} = 325 nm) excitation may provide comprehensible information about the effect of SPR on ZnO band structure. Fig. 4(b and c) show the O *K* -edge XANES spectra of ZnO/Au/Qz and ZnO/Qz samples, respectively, with and without laser excitation. The difference (with and without laser excitation) XANES spectra are shown at the bottom panel. Fig. 4(d) shows the net absorption of O *K*-edge XANES spectra of ZnO/Au/Qz and ZnO/Qz samples, respectively, with and without laser excitation. In ZnO/Au/Qz films the absorption intensity increases exponentially with

decreasing of ZnO film thickness, which indicates that transfer of electrons from ZnO to Au. Whereas in ZnO/Qz films the intensity decreases with the decrease of ZnO thickness. From these spectra it is clear that, the SPR of Au NPs has considerable effect on O 2*p* orbitals and the effect decrease with increase of ZnO film thickness. Fig. 5 shows the Au L_3-edge XANES spectra of thin and thinnest ZnO/Au/Qz samples with and without UV laser excitation. (In thickest film, the ZnO film thickness is larger than the probing sensitivity of X-ray, so measuring Au L_3-edge XANES in this film is not advisable). The features are attributed to the transition from Au $2p_{3/2}$ to 5*d*/6*s* states.[39] The difference XANES (with and without laser excitation) spectra are shown at the bottom panel of Fig. 5. With laser excitation the intensity of the Au L_3-edge XANES features reduced, which indicates that occupation of Au 5*d*/6*s* states due to transfer of electrons from ZnO to Au.

It should be noted that the enhanced intensity of O *K*-edge XANES features, of thinnest film, with laser excitation also show that large number of electrons transferred from ZnO to Au. Mainly these electrons are trapped in the surface states or defect levels within the ZnO bandgap.[40] During PL process, these electrons are again excited by the SPR of Au NPs with the interaction of incident light. Since, the energy of these excited electrons is higher than the ZnO bandgap.[41,42] these electrons are transferred to the conduction band of ZnO and increase the population. The enhanced population at conduction band increases the probability of radiative recombination with the valence band holes.

Fig. 6 displays the schematic diagram to illustrate the above mentioned mechanism. Fig. 6(a) shows that the trapping of excited electron by the defect levels just below the conduction band (CB). These trapped electrons relaxes via emitting phonons and then recombines with valence band hole by emitting defect emission. Fig. 6(b) shows that in the presence of Au NPs, the electrons in the defect levels jump to the Au Fermi level, as the photon energy of defect emission is very close to the SPR of Au NPs.[43,44] Thus, the electrons, from the ZnO

defect level, flow into the Au Fermi level. These electrons again excited due to SPR of Au NPs with the interaction of incident photon. Since the energy of these hot electrons is higher than the CB of ZnO, they can transfer back to the conduction band of ZnO.[14,45] Our XANES analyses at the O *K*-edge and Au *L*-edge also confirms the aforesaid processes. Thus the population at the ZnO CB is increased, which in turn increases the probability for radiative recombination with the valence band holes and results enhanced band-edge emission.

Even though the thickest ZnO/Au/Qz film exhibits more unoccupied states than the ZnO/Qz film (top panel of Fig. 4(a)), the PL intensity is same for both samples. This might be due to weak strength of the evanescent field of SPR of Au NPs and more defects in this film as evidenced from UV-visible absorption. Since the ZnO deposition conditions are identical in each set of films and the only difference in each set is the presence of Au NPs at the interface between ZnO and substrate, the factors affecting the effective coupling of the evanescent wave with the band structure of ZnO is mainly the exponential decay nature of evanescent wave with the increase of film thickness.[26] Further, the presence of defects in the film is also unavoidable concerning the factors affecting the band-edge emission. Because of these defects, the excited electrons are trapped and recombine via non-radiative mechanism due to strong EPC as evidenced from Raman analysis. In case of thin and thinnest films, due to less defects and weak EPC, the evanescent wave of SPR is effectively coupled to the ZnO band electrons and enhances the PL intensity via increasing the population at ZnO conduction band. Thus the exponential decay of SPR field strength and defects are the main factors affecting the PL intensity of ZnO/Au hybrids.

Conclusion

Electronic structure and optical properties of ZnO(*y* nm)/Au(10 nm) hybrid films, with y = 20, 50 and 150, have been investigated for effective coupling of SPR of Au NPs with ZnO band structure for enhanced optical properties. The surface states/defect density in ZnO film

plays an important role for effective coupling of SPR of Au NPs via electron-phonon coupling. The surface states/defect density in ZnO film plays an important role for effective coupling of SPR of Au NPs. In case of thin and thinnest films, the defect concentration (traps) is less and these defects are effectively passivated by the SPR of Au NPs, which enhances band edge emission and suppresses the defect emission. In case of thickest films, the exponential decay of SPR induced local field and defects in the film are the main factors affecting the coupling of SPR with the ZnO band structure. The local electronic structure analysis at O *K*-edge reveals that, in thinnest film more unoccupied states are introduced in ZnO due to hybridization of O 2*p* and Au 5*d*/6*s* orbitals. In other words, electrons in the defect states are pumped via SPR of Au NPs to the conduction band of ZnO. The increased density of states causes the enhanced optical properties of ZnO/Au hybrid films via increasing the population at the excited state of ZnO.

Acknowledgements

The authors K.S., D.K.A. and D.K. would like to acknowledge the Department of Science and Technology (DST), Govt. of India for providing the XRD facility to IUAC through the IRPHA project. The authors K.S. and W.F.P. would like to acknowledge the Ministry of Science and Technology, Taiwan for providing the financial support.

References

1. K. Okamoto, I. Niki, A. Shvartser, Y. Narukawa, T. Mukai, and A. Scherer, Nat. Mater. **3**, 601 (2004).
2. E. Ozbay, Science **311**, 189 (2006).
3. N. Gogurla, A. K. Sinha, S. Santra, S. Manna and S. K. Ray, Sci. Rep. **4**, 6483 (2014).
4. C. H. Ahn, K. Senthil, H. K. Cho and S. Y. Lee, Sci. Rep., 2013, **3,** 2737.
5. Z. Jin, L. Gao, Q. Zhou and J. Wang, Sci. Rep., 2014, **4,** 4268.
6. A. Asok, M. N. Gandhi and A. R. Kulkarni, Nanoscale, 2012, **4**, 4943.
7. C. Drouilly, J.-M. Krafft, F. Averseng, S. Casale, D. B. Bachi, C. Chizallet, V. Lecocq, H. Vezin, H. L. Pernot, and G. Costentin, J. Phys. Chem. C 2012, **116**, 21297.
8. C. W. Lai, J. An, and H. C. Ong, Appl. Phys. Letts., 2005, **86,** 251105.
9. Y. Harada, I. Tanahashi and N. Ohno, J. Lumin., 2009, **129,** 1759.
10. B. J. Lawrie, R. F. Haglund Jr and R. Mu, Opt. Express, 2009, **17,** 2565.
11. K. Saravanan, B. K. Panigrahi, R. Krishnan and K. G. M. Nair, J. Appl. Phys., 2013, **113**, 033512.
12. N. Gogurla, A. K. Sinha, S. Santra, S. Manna and S. K. Ray, Sci. Rep., 2014, **4,** 6483.
13. D. Zhang, H. Ushita, P. Wang, C. Park, R. Murakami, S. Yang and X. Song, Appl. Phys. Lett., 2013, **103,** 093114.
14. C. W. Cheng, E. J. Sie, B. Liu, C. H. A. Huan, T. C. Sum, H. D. Sun and H. J. Fan, Appl. Phys. Lett., 2010, **96,** 071107.
15. X. Su, S. F. Y. Lib and S. J. O'Shea, Chem. Commun., 2001, 755-756.
16. P. Galletto, P. F. Brevet, H. H. Girault, R. Antoineb and M. Broyer, Chem. Commun., 1999, 581–582.

17. *Handbook of Modern Ion Beam Materials Analysis*, Edited by J. R. Tesmer and M. Nastasi, Materials Research Society, Pittsburgh, Pennsylvania, 1995.
18. M. Mayer, SIMNRA user's guide. Tech. Rep. IPP 9/113, Max-Planck-Institut für Plasmaphysik, Garching, 1997.
19. N. Ashkenov, B. N. Mbenkum, C. Bundesmann, V. Riede, M. Lorenz, D. Spemann, E. M. Kaidashev, A. Kasic, M. Schubert, M. Grundmann, G. Wagner, H. Neumann, V. Darakchieva, H. Arwin, and B. Monemar, J. Appl. Phys., 2003, **93,** 126.
20. V. A. Fonoberov and A. A. Balandin, Phys. Rev. B, 2004, **70,** 233205.
21. K. A. Alim, V. A. Fonoberov and A. Balandin, Appl. Phys. Lett., 2005, **86,** 053103.
22. T. Sakano, Y. Tanaka, R. Nishimura, N. N. Nedyalkov, P. A. Atanasov, T. Saiki and M. Obara, J. Phys. D: Appl. Phys., 2008, **41,** 235304.
23. H. Sun, M. Yu, G. Wang, X. Sun and J. Lian, J. Phys. Chem. C, 2012, **116,** 9000.
24. P. K. Giri, S. Bhattacharyya, D. K. Singh, R. Kesavamoorthy, B. K. Panigrahi and K. G. M. Nair, J. Appl. Phys., 2007, **102**, 093515.
25. H. M. Cheng, K. F. Lin, H. C. Hsu, C. J. Lin, L. J. Lin and W. F. Hsieh, J. Phys. Chem. B, 2005, **109,** 18385.
26. W. L. Barnes, A. Dereux and T. W. Ebbesen, Nature, 2003, **424,** 824.
27. *UV spectroscopy, Techniques, instrumentation, data handling,* Edited by B. J. Clark, T. Frost and M. A. Russell, Chapman and Hall, London, 1993.
28. H. Seo, C. J. Park, Y. J. Cho, Y. B. Kim and D. K. Choi, Appl. Phys. Lett., 2010, **96**, 232101.
29. X. Hou, L. Wang, G. He and J. Hao, Cryst. Eng. Comm., 2012, **14,** 5158.
30. C. Chen, H. He, Y. Lu, K. Wu and Z. Ye, Appl. Mater. Interfaces, 2013, **5,** 6354.
31. X. Gu, T. Qiu, W. Zhang, P. K. Chu, Nanoscale Res. Lett., 2011, **6,** 199.

32. Y. Lin, C. Xu, J. Li, G. Zhu, X. Xu, J. Dai and B. Wang, Adv. Optical Mater., 2013, **1,** 940.

33. J. T. Thienprasert, S. Rujirawat, W. Klysubun, J. N. Duenow, T. J. Coutts, S. B. Zhang, D. C. Look and S. Limpijumnong, Phys. Rev. Lett., 2013, **110,** 055502.

34. S. L. Shi, G. Q. Li, S. J. Xu, Y. Zhao and G. H. Chen, J. Phys. Chem. B, 2006, **110,** 10475.

35. S. Ramanathan, S. Bandyopadhyay, L. K. Hussey and M. Muñoz, Appl. Phys. Lett., 2006, **89,** 143121.

36. D. Das and P. Mondal, RSC Adv., 2014, **4,** 35735.

37. M. Subramanian, P. Thakur, S. Gautam, K. H. Chae, M. Tanemura, T. Hihara, S. Vijayalakshmi, T. Soga, S. S. Kim, K. Asokan and R. Jayavel, J. Phys. D: Appl. Phys., 2009, **42,** 105410.

38. R. A. Rosenberg, G. K. Shenoy, L.-C. Tien, D. Norton, S. Pearton, X. H. Sun and T. K. Sham, Appl. Phys. Lett., 2006, **89,** 093118.

39. J. W. Chiou, S. C. Ray, H. M. Tsai, C. W. Pao, F. Z. Chien, W. F. Pong, M.-H. Tsai, J. J. Wu, C. H. Tseng, C.-H. Chen, J. F. Lee and J.-H. Guo, Appl. Phys. Lett., 2007, **90,** 192112.

40. L. Ke, S. C. Lai, J. D. Ye, V. L. Kaixin and S. J. Chua, J. Appl. Phys., 2010, **108**, 084502.

41. X. Li, Y. Zhang and X. Ren, Opt. Exp., 2009, **17,** 8735.

42. J. M. Lin, H. Y. Lin, C. L. Cheng and Y. F. Chen, Nanotechnology, 2006, **17,** 4391.

43. X. Yong and A. A. S. Martin, Am. Mineral., 2000, **85,** 543.

44. H. Y. Lin, C. L. Cheng, Y. Y. Chou, L. L. Huang, Y. F. Chen and K. T. Tsen, Opt. Express, 2006, **14,** 2372.

45. L. Liu, H. Yang, X. Ren, J. Tang, Y. Li, X. Zhang and Z. Cheng, Nanoscale, 2015, **7**, 5147.

Figure captions

Fig. 1 Rutherford backscattering spectrometry spectra of all ZnO/Au/Qz and ZnO/Qz samples. The open symbols are the experimental data and the solid lines are the simulated curve. The insets show the typical cross-sectional TEM image of the films. The inset (I) shows the surface topography of the Au film deposited on quartz substrate, analyzed by AFM.

Fig. 2 (a) GIXRD pattern of thickest and thinnest sets of ZnO/Au/Qz and ZnO/Qz samples. The ZnO crystals are preferentially oriented in (002) direction and the formation of fcc structured Au NPs also seen in the pattern. (b) Raman scattering spectra of all samples. The ZnO deposited with Au film have shown enhanced signal in comparison with that of ZnO directly deposited on quartz. The inset shows ratio of 2 LO to 1 LO modes.

Fig. 3 (a) UV-Visible absorption spectra. The absorption peak around 365 nm corresponds to the band gap of ZnO. The thickest ZnO/Qz film shows a broad absorption band in the region 500 – 800 nm due to the presence of defects in the film. The ZnO/Au/Qz samples exhibit an additional absorption peak around 600 nm due to the SPR of Au NPs. (b) PL spectra in the UV region. In thickest film no enhancement observed whereas in thin film clear enhancement is observed in the presence of Au film and is pronounced in thinnest film. (c) PL spectra in the visible region. In thickest film, the intensity is almost same in both samples. In thin films, the visible emission is suppressed in the presence of Au film and is almost completely suppressed in thinnest film in the presence of Au film. (d) The enhancement ratio of UV emission and suppression ratio of visible emission as a function of ZnO film thickness.

Fig. 4 (a) O *K*-edge XANES spectra recorded at glancing incident angle in TEY mode. (b) and (c) O *K*-edge XANES spectra of ZnO/Au/Qz and ZnO/Qz samples, respectively,

with and without laser excitation. The difference XANES (with and without laser excitation) spectra are shown at the bottom panel. (d) The net absorption of O *K*-edge XANES spectra of ZnO/Au/Qz and ZnO/Qz samples, respectively, with and without laser excitation.

Fig. 5 The Au L_3-edge XANES spectra, recorded in TFY mode, of ZnO(20nm)/Au/Qz and ZnO(50nm)/Au/Qz samples, respectively, with and without UV laser excitation. The difference XANES signal is shown at the bottom panel.

Fig. 6 Schematic diagrams of PL process in (a) ZnO film and (b) ZnO/Au hybrid films. In ZnO film, the excited electrons trapped by the defect levels just below the conduction band. These trapped electrons relaxes via emitting phonons and then recombines with valence band hole by emitting defect emission. Whereas in ZnO/Au hybrid films, the defect level electrons jump to the Au Fermi level, and again excited by SPR with the interaction of incident photon. Then these electrons are transferred to the conduction band of ZnO and increase the population, which in turn increases the probability for radiative recombination with the valence band holes and enhances the band-edge emission.

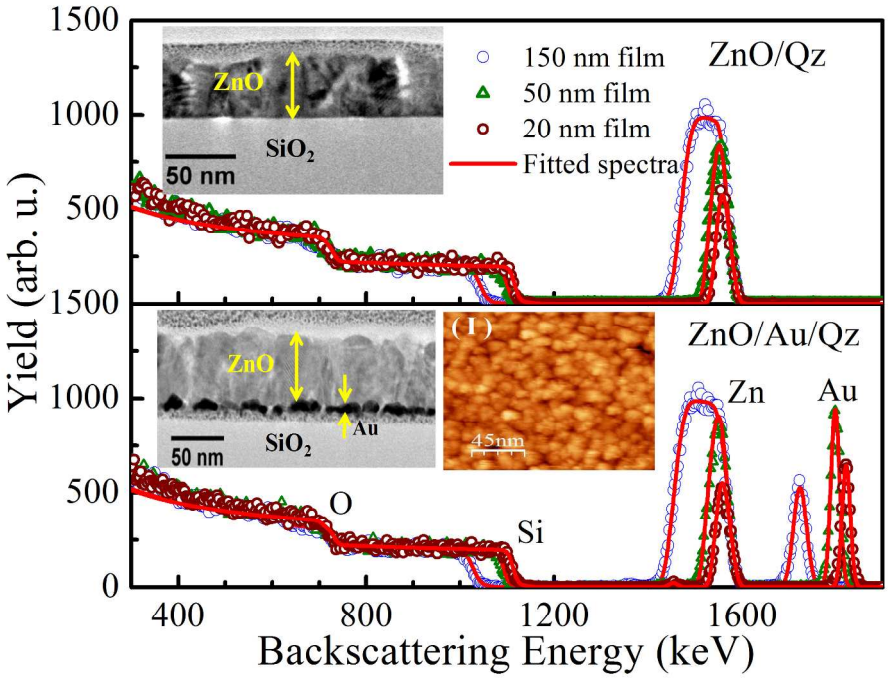

508x389mm (150 x 150 DPI)

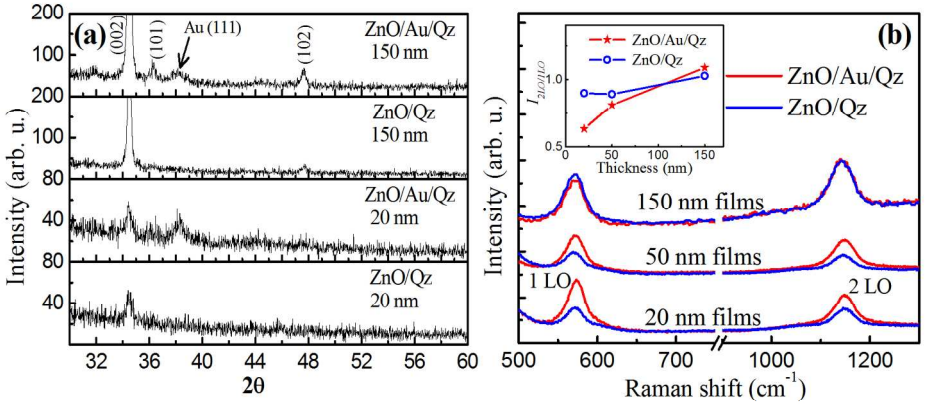

508x389mm (100 x 100 DPI)

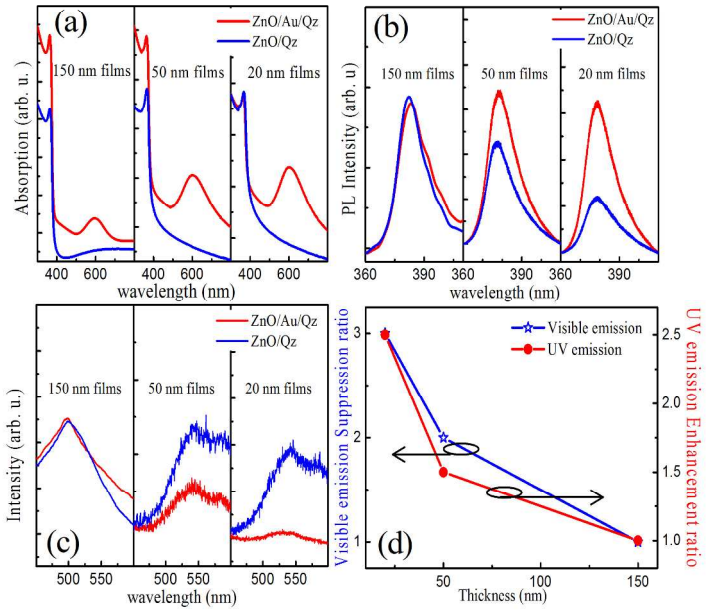

508x389mm (150 x 150 DPI)

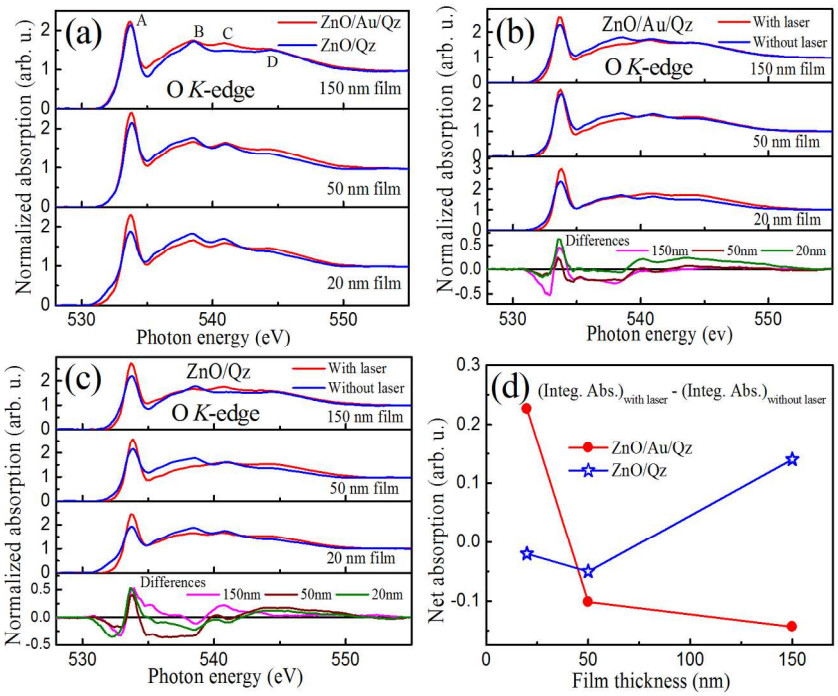

508x389mm (100 x 100 DPI)

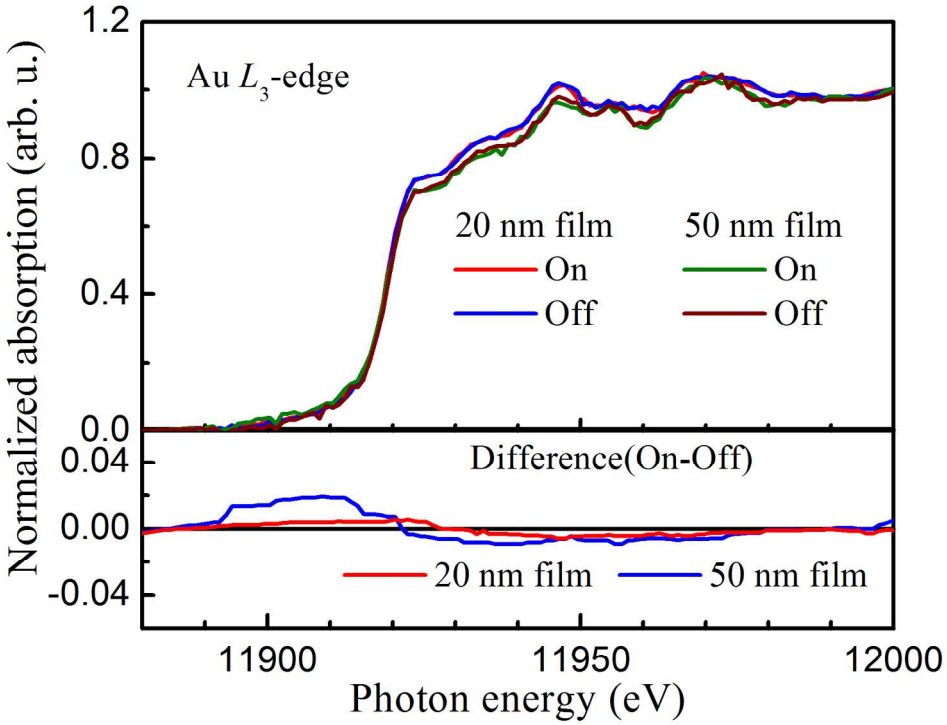

508x389mm (100 x 100 DPI)

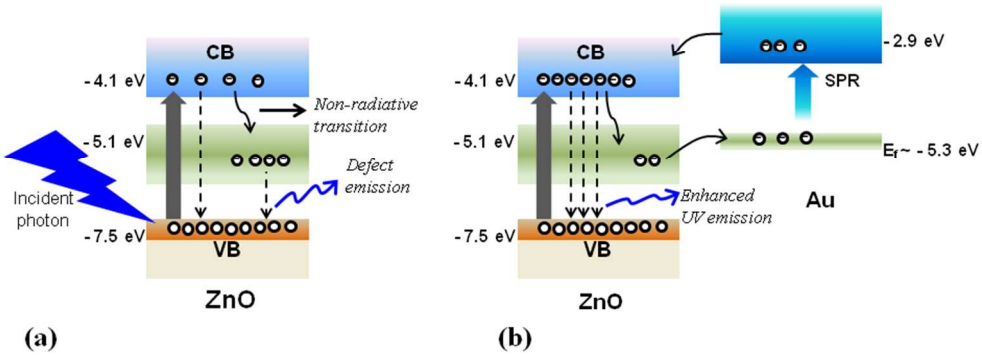

254x190mm (96 x 96 DPI)

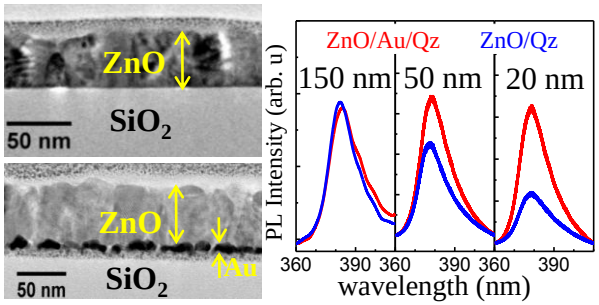

Thickness and defects effects on the optical properties of ZnO/Au hybrid films were studied using optical and electronic structural studies.

Graphical abstract